Journal of Applied Polymer Science

Physical Properties of Poly Lactic Acid/Clay Nanocomposite Films: Effect of Filler Content and Annealing Treatment

Pietro Russo,[1] Sara Cammarano,[2,3] Emiliano Bilotti,[2] Ton Peijs,[2,4] Pierfrancesco Cerruti,[1] Domenico Acierno[3]

[1]Institute of Chemistry and Technology of Polymers—CNR, Via Campi Flegrei 34, 80078 Pozzuoli, Italy

[2]Queen Mary University of London, Centre for Materials Research & School of Engineering and Materials Science, Mile End Road E1 4NS, London, United Kingdom

[3]Department of Chemical, Materials Engineering and Industrial Production – University of Naples Federico II – P.le V. Tecchio 80, 80125 Naples, Italy

[4]Eindhoven University of Technology, Eindhoven Polymer Laboratories, PO Box 513, 5600 MB Eindhoven, The Netherlands

Correspondence to: P. Russo (E-mail: pietro.russo@unina.it)

ABSTRACT: Polylactic acid (PLA)-based nanocomposite films, containing up to 5% by weight of two types of nanoclays: sepiolite needle-like clay and halloysite nanotube clay, were prepared via industrially viable melt processing route. Clays modify the crystallinity of the hosting PLA affecting its gas barrier and mechanical properties. Annealing treatments of composite films were found to be critical in the optimization of these properties with an additional enhancement in crystallinity and stiffness especially in presence of clays. © 2013 Wiley Periodicals, Inc. J. Appl. Polym. Sci. **2014**, *131*, 39798.

KEYWORDS: films; clay; mechanical properties; structure–property relations; thermal properties

Received 9 May 2013; accepted 31 July 2013

DOI: 10.1002/app.39798

INTRODUCTION

In the last few decades, environmental issues have stimulated the development of plastic items based on so-called bioplastics as promising alternatives to conventional petroleum-derived resins. However, for many years, the high production costs and relatively poor performances of bioplastics have severely limited their applications to specific high value fields as the medical one.

Recently, the development of new technologies and the expansion of the scale of production have allowed extending the spectrum of industrial applications of these materials to new areas including textiles and packaging fields.

Among other bioplastics, polylactic acid (PLA) has attracted particular interest. PLA is an aliphatic, thermoplastic and biodegradable polyester that is produced by processes of fermentation and distillation of starch (mainly corn).[1–10] Products based on PLA are particularly suitable for applications in which recyclability is not operable, or too complex/expensive—such as in the case of agricultural mulching—or when controlled degradability is desired—as in the case of degradable implants. Moreover, PLA is recognized as GRAS (Generally Recognized as Safe), which makes it suitable for food packaging uses, especially in consideration of its compostability (e.g. PLA packaging can be composted together with out of date foods). Conversely, PLA suffers from few shortfalls including poor barrier properties, low thermal stability, and limited toughness.

The focus of this work is the improvement of barrier properties of PLA films via two different approaches: addition of nanoclay and thermal annealing.

Nanoclays, most commonly platelet-like montmorillonite clays, have already shown to improve barrier properties of PLA. Recently Picard et al.[11] showed a decrease in PLA film permeability with addition of organo-modified MMT, which was interpreted in terms of Nielsen law and explained by an increase in tortuosity path.

In this work two different nanoclays have been considered, for the first time, with regards to barrier properties improvement: sepiolite needle-like clay and halloysite nanotube clay.

These two clays offer an interesting model case because of their shape: needle and tube (1D) as opposed to the more common platelet-like shape (2D) of montmorillonite.

Halloysite nanotubes (HNT) is an alumina-silicate clay with the empirical formula $Al_2Si_2O_5(OH)_4$. HNT can entrap—either in

© 2013 Wiley Periodicals, Inc.

its inner lumen or within spaces of aluminosilicates shells—a wide range of active agents, such as drugs and marine biocides.[12–15]

Sepiolite is a layered hydrated magnesium silicate ($Si_{12}O_{30}Mg_8(OH)_4\cdot(H_2O)4\cdot 8H_2O$) characterized by a needle like morphology based on alternated blocks of tunnels in the fiber direction. Sepiolite clay has been reported to improve mechanical,[12–16] rheological,[17] and thermal[18] properties of a wide range of polymers.

The effect of nanoclay addition to the barrier properties of PLA films has been compared with the simple effect of thermal annealing. Annealing treatments are usually an efficient way to increase modulus, tensile strength and to reduce gas permeability, as a consequence of the reduced free volume and increased crystallinity of the polymer. This is particularly valid in the case of PLA as this matrix, like most other polyesters, shows a slow crystallization rate.[19,20]

EXPERIMENTAL

Materials

In this work PLA2002D, average molecular weight 121.400 g/mol, from NatureWorks (Minneapolis MN, USA), was used as a matrix. According to the supplier this grade is characterized by a D-lactide content of 4.25%, a residual monomer content of 0.3% and a density of 1.24 g/cm^3 and it is specifically designed for extrusion and thermoforming applications.

Pangel sepiolite clay were supplied by Tolsa (Madrid, Spain). This clay is characterized by a bulk density of 30 g/L, a BET surface area of 320 m^2/g, and an aspect ratio of 20–100.

Halloysite G produced by Atlas Mining, Nanoclay Technology Division, was purchased from Sigma-Aldrich. This clay, has an average tube diameter of 50 nm and an inner lumen diameter of 15 nm. Other interesting properties are: specific surface area of 65 m^2/g, a pore volume of $\sim$ 1.25 mL/g, a refractive index of 1.54, and a specific gravity of 2.53 g/cm^3.

In this research only pristine clays have been considered. It is known that some surface modifications of nanoclay could improve their dispersion in PLA but, on the other hand, have detrimental effects on other performance as the water vapour permeability.

Film Sample Preparation

PLA pellets and the two nanoclays were dried overnight at 80°C before extrusion.

Nanocomposites were prepared using a mini twin-screw extruder (DSM X'plore Micro 15), under nitrogen, at 190°C and a screw speed of 200 rpm, for 5 min. Masterbatches loaded with 15% by weight of each of the two clays were first prepared and then diluted by the addition of pure PLA to obtain concentrations of 0.1, 0.5, 1.0, 3.0, and 5.0 wt % of each type of clays (sepiolite or halloysite).

The neat matrix, processed under the same conditions has been always considered as the reference material during characterization stages.

Finally, extruded materials, after being palletized and predried overnight at 80°C, were compression moulded at 190°C into films, with an average thickness of about 100 μm, using a Lab-Tech hydraulic press mod. LP420B.

The resulting films were conditioned at 80°C overnight to assess influences of annealing on their physical properties. The choice of this temperature was based on indications already reported in the literature.[20]

Characterizations

Cryo-fractured cross-sectional surfaces, prepared by the immersion of films in liquid nitrogen, were observed by scanning electron microscopy (SEM). Collected micrographs showed the actual dispersion of sepiolite and halloysite in the PLA matrix. At this regard, a Jeol JSM-6300F SEM was used to analyze gold-coated samples.

Differential scanning calorimetry (DSC) and thermo gravimetric analysis were used to study the thermal properties of the nanocomposites.

In particular, calorimetric measurements were performed with a DSC Mettler-Toledo 822e on samples with a weight of 4–6 mg. Samples were heated from room temperature to 230°C at a ramp rate of 10°C/min, kept at this temperature for 5 min to remove any previous thermal history, then cooled to 30°C at the rate of 10°C/min and subsequently heated again to a temperature of 230°C. Information on degree of crystallinity (X_c), glass transition temperature (T_g), melting temperature (T_m), and crystallization temperature (T_c) of all materials were determined.

Thermo gravimetric analysis was conducted on a TA Instruments Q500e. Each specimen was heated from 40°C to 600°C under nitrogen flow and from 600°C to 750°C in air with a ramp rate of 10°C/min. The average initial mass of samples was approximately equal to 5 mg.

Water vapour permeability tests were performed on each PLA-based films by means of ExtraSolution Multiperm equipment, operating at 25°C and 50% relative humidity (RH), always taking the neat PLA film as the reference sample. The exposed area of the film was 50 cm^2. Collected data were converted into water vapour transmission rate (WVTR) corresponding to the flux of vapor flow between two parallel surfaces under steady conditions at a specific temperature and RH. The permeability coefficient P was calculated multiplying WVTR by film thickness and dividing by water vapor partial pressure in the bottom chamber (1586 Pa). Diffusion coefficients D were obtained according to the following equation:

$$D = L^2/6t$$

with L being the thickness of the film. The time lag, t, was obtained by extrapolation from the integral curves of the experimental oxygen flux signals versus time.[24] At least three tests were conducted for each film sample in order to confirm the reproducibility of the data.

Water absorption tests were also carried out, according to the standard ASTM *D 570*. Specimens were cut into squares of 3 $\times$ 3 cm^2 and annealed in an oven at 80°C for 24 hours. Before being tested, specimens were stored into a desiccator at room temperature for 24 hours. After immersion in distilled water for

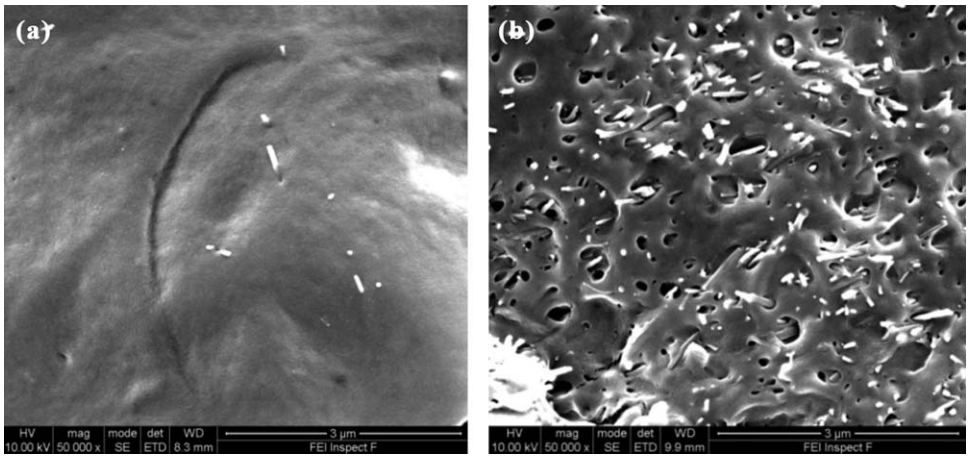

Figure 1. SEM micrographs of: (a) PLA / 0.1 wt % sepiolite and (b) PLA / 5 wt % sepiolite.

24 hours at room temperature, specimens were wiped dry and then immediately weighted using an analytic balance with an accuracy of 0.1 mg. After immersion and measurement of mass, each specimen was reconditioned using the initial drying condition to determine any mass loss because of water degradation.

Water absorption was calculated by the increase in weight divided by the specimen average thickness.

Finally, tensile tests were performed according to a modified ASTM D882 with a universal testing machine (Instron 5566), using a 1-kN load cell, standard grips, and at 5 mm/min test speed. At least 10 dumbbell-shaped specimens for each investigated film samples were cut with a puncher from the 100-μm thick films and tested. Average values are reported.

RESULTS AND DISCUSSION

Morphological observations of fractured surfaces of composite films showed a good dispersion of sepiolite up to 3% by weight. Higher loading with the formation of micrometric aggregated for higher loadings [see Figures 1(a,b)]. The good dispersion at relatively low filler contents could be ascribed to the occurrence of a good interaction between the ester groups of PLA and sylanol groups (Si-OH) on sepiolite.

On the contrary, the morphological analysis of PLA/halloysite composites [see Figures 2(a,b)] has shown a poor dispersion with evident presence of aggregates even for the content of 3 wt % as well as a clear fragmentation of HNT easily related to the fragility of the clay walls, unable to withstand the thermo-mechanical stresses applied during the melt compounding process.

In Figure 3(a) typical comparison between DSC thermograms, (second heating) before and after annealing of PLA+1 wt % sepiolite film is reported.

Thermal properties including glass transition, cold crystallization, and melting temperatures (T_g, T_{cc}, and T_m) of all examined films and their degree of crystallinity (X_c) are summarized in Tables I and II, for halloysite and sepiolite filled samples, respectively. The evaluation of the crystallinity was based on the difference between the melting and cold crystallization enthalpies, taking the melting enthalpy of 100% crystalline PLA equal to 93.1 J/g.[21]

Before annealing, in all cases an exothermic relaxation, usually attributed to the nonequilibrium microstructure of films, has been observed after the glass transition temperature (at approximately 57°C).

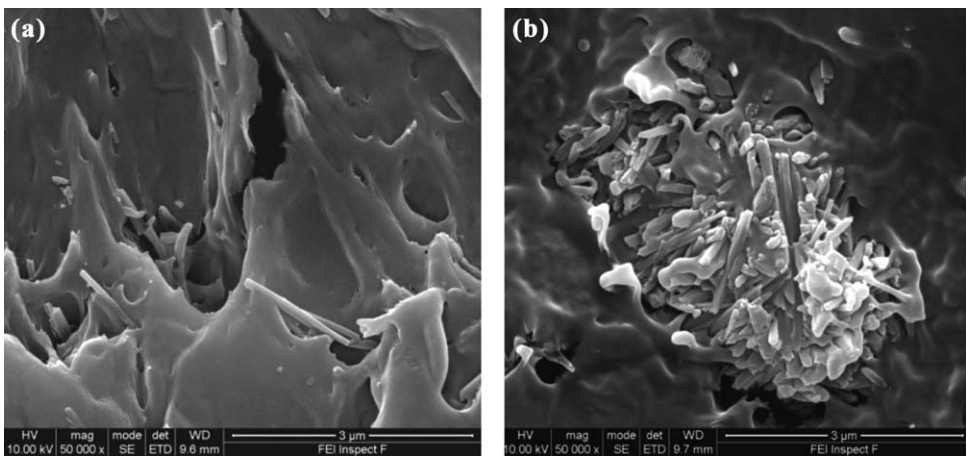

Figure 2. SEM topography of: (a) PLA /1 wt % halloysite and (b) PLA / 3 wt % halloysite.

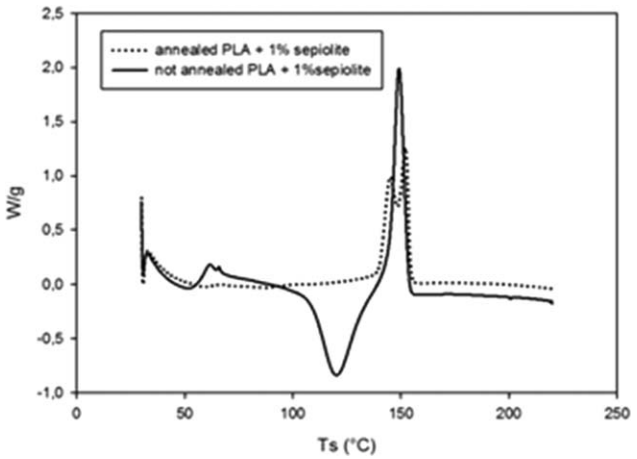

Figure 3. DSC scan of PLA samples 1 wt % of sepiolite, before and after annealing treatment.

Calorimetric data showed an increase of crystallinity, especially after the annealing of samples, whereas the cold-crystallization of the matrix, slightly shifted to higher temperatures for formulations with very low contents of fillers, disappeared by further increase of clays' content. This behavior, usually ascribed to nucleating effects induced by the filler, seemed to be reduced for loadings higher than 1% by weight, probably for the formation of aggregates as already confirmed by the morphological analysis.

Another interesting phenomenon is the appearance of a double melting peak for annealed PLA samples containing 0.1, 0.5, and 1.0 wt % of sepiolite. This phenomenon is widely reported in the literature and explained by the formation of two different crystalline structures: the α-form with a pseudo-orthorhombic structure, melting at higher temperature and more stable than the β-form, having an orthorhombic structure and melting at lower temperature.[18]

Thermogravimetric results are summarized in Table III, in which parameters such as the temperature of incipient thermal degradation ($T_{5\%}$), the temperature at which the rate of weight loss is the highest ($T_{max,\ DTG}$) and the weight percent of residue in air at 750°C are reported *for all the investigated film samples.*

Clearly, the halloysite addition leads to a decrease in PLA thermal stability. This effect is enhanced with the clay content. These results have been explained invoking catalytic phenomena reported by Kopinke et al.[22] who suggested the occurrence of a radical reaction starting with alkyloxigen or acyl-oxigen homolysis, forming carbon monoxide and several types of oxygen-centerd and carbon-centerd radicals. This behavior could be emphasized by a reduced contact surface area between polymeric matrix and clay because of the formation of aggregates, confirmed by SEM micrographs.

On the other hand, the onset of thermal degradation for PLA/sepiolite composites seems to be slightly higher than that of neat PLA and it increases with the amount of nanoclay, leading to a maximum increase in thermal stability of approximately 6°C. This behavior is explained by the presence of silicates acting as an insulating barrier and the labyrinth effect because of the dispersion of clays in the nanocomposites, involving to a

Table I. DSC Data for Different Amounts of HNT in PLA

	Annealed				*Nonannealed*
Sample	T_g (°C)	T_{cc} (°C)	T_m (°C)	X_c (%)	X_c (%)
PLA	57.8	133.3	150.4	18.1	2.7
0.1 wt % HNT	56.8	134.3	150.8	18.2	2.6
0.5 wt % HNT	58.2	-	152.3	23.3	3.5
1 wt % HNT	57.3	-	152.3	24.7	4.7
3 wt % HNT	57.8	-	151.9	23.2	3.2
5 wt % HNT	56.8	-	152.6	20.1	4.3

Table II. DSC Data for Different Amounts of Sepiolite in PLA

	Annealed					*Nonannealed*
Sample	T_g (°C)	T_{cc} (°C)	T_{m1} (°C)	T_{m2} (°C)	X_c (%)	X_c (%)
PLA	57.8	133.3	-	150.4	18.1	2.7
0.1 wt % SEP	56.7	133.3	142.3	150.4	18.3	2.6
0.5 wt % SEP	57.2	133.9	144.2	150.7	15.1	6.7
1 wt % SEP	57.4	-	144.1	152.2	27.1	5.0
3 wt % SEP	57.1	-	-	150.8	20.6	4.5
5 wt % SEP	59.9	-	-	152.3	24.5	4.4

Table III. Thermogravimetric Parameters of all Investigated Materials

Sample	$T_{5\%}$	$T_{max,\ DTG}$	Residue at 750°C (%)
PLA	342 ± 1	379 ± 2	0
0.1 wt % HNT	342 ± 1	380 ± 1	0.11
0.5 wt % HNT	343 ± 1	390 ± 1	0.64
1 wt % HNT	341 ± 2	379 ± 2	0.73
3 wt % HNT	328 ± 2	377 ± 3	2.95
5 wt % HNT	326 ± 2	375 ± 2	4.71
0.1 wt % SEP	341 ± 1	379 ± 1	0.07
0.5 wt % SEP	345 ± 2	379 ± 1	0.48
1 wt % SEP	347 ± 2	379 ± 2	1.31
3 wt % SEP	348 ± 2	382 ± 2	3.15
5 wt % SEP	348 ± 2	381 ± 2	5.00

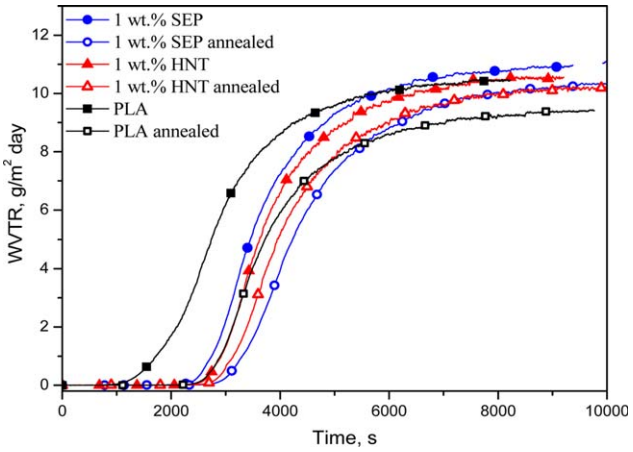

Figure 4. WVTR of untreated and annealed neat PLA, PLA/1 wt % HNT, and PLA/1 wt % SEP. [Color figure can be viewed in the online issue, which is available at wileyonlinelibrary.com.]

delay in the volatilization process. According to Wu et al.[23] the improved thermal stability can be attributed to the ability of clays to reorganize themselves creating a physical barrier on the PLA surface. However, the mechanism governing the increase in thermal stability of the nanocomposites needs further investigation and work is in progress to explore this aspect.

Figure 4 reports the water vapor transmission rate (WVTR) as a function of the time (t) for annealed and nonannealed films based on neat PLA, PLA containing 1 wt % of halloysite, and PLA filled with 1 wt % of sepiolite. Processing of these data has allowed to evaluate some transport parameters as permeability, diffusion, and solubility coefficients for PLA and PLA /1 wt % clay nanocomposites before and after annealing.

It can be observed that the permeability of composite films is slightly higher than that of the neat PLA based ones. This result can be mainly attributed to the hydrophilicity of the fillers, as confirmed by the higher values of water vapor solubility coefficients displayed by the composites with respect to neat PLA samples. A similar result was reported by Rhim et al.,24 who found that the presence of unmodified natural nanoclay Cloisite Na^+ increased the permeability of PLA films because of the hydrophilicity of the filler.

On the other hand, the positive effect of the presence of nanoclays on the polymer barrier properties is demonstrated by the diffusion coefficients values, which are about 15% lower for both composite films with respect to the pure polymer. A similar behavior has been recently described for PLA nanocomposites containing HNT, which showed a decrease of diffusion coefficients by about 12% upon addition of 3 wt % of nanofiller.[25] This outcome is generally attributed to the tortuous path for water vapor diffusion because of the filler particles distributed in the polymer matrix, which increase the effective diffusion path length.[24]

As far as the effect of the annealing is concerned, it can be observed that both WVTR and permeability values of neat PLA are reduced by approximately 10% after the thermal treatment, as a consequence of increased crystallinity and reduced free volume of the matrix. This behavior is mainly related to the significant increase of the time needed for water vapor to diffuse across the film. Table IV indeed shows that the WV diffusion coefficient of the annealed PLA is more than 20% lower in comparison to the untreated polymer. This finding can be explained by the increase in crystallinity measured by DSC measurements after annealing, as higher polymer crystallinity reduces permeability of water. Usually crystallites reduce the cross-sectional area for diffusion, increasing the diffusion path length, even imposing significant restraints on the mobility of the amorphous phase.[26]

Less pronounced changes in WVTR and permeability values are brought about by annealing composites filled with 1 wt % of

Table IV. WVTR and Permeability Data of Neat PLA and Nanocomposites

Sample	WVTR (g 24h^{-1} m^{-2})	Permeability × 10^{12} (g m m^{-2} s^{-1} Pa^{-1})	Diffusion × 10^6 (m^2 s^{-1})	Solubility × 10^6 (g m^{-3} Pa^{-1})
PLA	10.4 ± 0.4	6.3 ± 0.2	3.8 ± 0.2	1.7 ± 0.2
PLA annealed	9.3 ± 0.2	5.7 ± 0.1	3.0 ± 0.1	1.9 ± 0.1
1 wt % HNT	10.6 ± 0.2	6.7 ± 0.1	3.2 ± 0.1	2.1 ± 0.1
1 wt % HNT annealed	10.2 ± 0.2	6.5 ± 0.2	3.0 ± 0.1	2.2 ± 0.1
1 wt % SEP	10.9 ± 0.2	6.9 ± 0.1	3.3 ± 0.1	2.1 ± 0.1
1 wt % SEP annealed	10.3 ± 0.1	6.5 ± 0.1	2.8 ± 0.1	2.3 ± 0.1

clays. In this case, the presence of the nanoclay inclusions results in a high lag time as a consequence of an enhanced tortuosity of diffusion paths to be faced by the permeant, and the influence of the annealing treatment is reduced. However, in the sepiolite-filled systems the effect of annealing on the lag time seems to be more pronounced in comparison to the halloysite-filled systems, and the diffusion coefficient of 1 wt % SEP is reduced by about 10% after annealing: behavior that has been ascribed to the massive increase in crystallinity observed for this sample after the thermal treatment.

Results in Table IV also indicate that for all samples, the solubility coefficient is relatively constant or slightly increasing because of annealing, regardless of the degree of crystallinity. Even for PLA, which shows the larger decrease in permeability after the thermal treatment, the value of the solubility coefficient is higher than that of nonannealed sample. This trend of the solubility coefficient is not easily predictable as, in general, the higher the crystalline fraction of a semicrystalline polymer, the lower the solubility.[27] However, a similar trend was found by Siparsky et al. who observed constant values of solubility for PLA samples with different crystallinity degrees.[28] This result was regarded as indicative of the existence of clustering in the PLA system, that is the ordered structuring of water within the polymer stabilized by hydrogen bonding between the water molecules. This phenomenon could also explain our experimental observation, however, some consideration about the polymer crystallinity may be also put forward. It was demonstrated that annealing PLA at temperatures below 95°C results in the formation of only the β crystalline phase.[29] The latter crystalline form is reported to have a looser and more disordered molecular packing within the unit cell than in the α form, because of the larger lattice dimension and weaker interchain interactions.[30] The conformational disorder of this crystalline phase suggests that it may show increased water solubility coefficients, which could explain the results observed for the PLA based samples annealed at 80°C.

Figure 5 shows the relative absorption versus nanoclay content of annealed samples. Relative absorption was calculated normalizing each absorption value of composites with respect to the same parameter evaluated for the pure PLA.

It is evident that the water absorption of PLA / sepiolite composites decreased with increasing nanoclay content up to 3 wt %. This effect has been attributed to the homogeneous dispersion of clays in these composite as was confirmed by SEM analysis. The improvement in barrier properties seems not to be strongly dependent on the increase in crystallinity and the correlation appears to be nonlinear. Further increase of the concentration above 3 wt % results in an opposite trend. This effect has been attributed to the formation of filler aggregates leading to a reduction of the polymer/clay interface and to the formation of morphological imperfections in which the water could be absorbed.

Halloysite-based composites, instead, show an increase in water absorption behavior also in correspondence of low filler content. This is probably because of the lower aspect ratio and poorer dispersion of halloysite. This result can be also explained by the ability of halloysite to trap water. Also regarding these aspects, structural investigations are in progress to support the invoked interpretations of WVTR results.

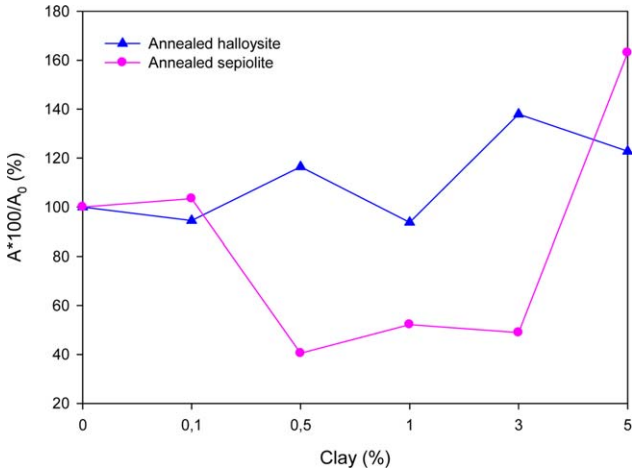

Figure 5. Relative water absorption. (A/A_o) versus nanoclay content for annealed nanocomposite samples. [Color figure can be viewed in the online issue, which is available at wileyonlinelibrary.com.]

Mechanical tensile properties for all film samples after the annealing treatment are reported in Table V. It is evident that, although the modulus unexpectedly seems to be unaffected by the applied annealing conditions and clays content, a relevant effect on the tensile strength of neat PLA is observed. Inclusion of nanofillers, again, shows only a minor influence on properties. In other words, it seems that the annealing treatment is dominant over the nanoclay effect.

Mechanical properties of PLA/halloysite samples start to decrease with filler content above a critical value probably because of the formation of aggregates.

Finally, pictures of PLA/sepiolite and PLA/halloysite composite films (Figure 6) evidence how the included fillers affect their

Table V. Young' Modulus (E), Ultimate Tensile Stress (σ), and Strain to Break (ε) of PLA / Hallosite Nanocomposite Films

Sample	E (GPa)	σ (MPa)	ε (%)
PLA nonannealed	3.7 ± 0.1	59.5 ± 4.8	10.1 ± 3.5
PLA annealed	3.7 ± 0.1	69.6 ± 2.7	5.1 ± 2.2
0.1 wt % HNT annealed	3.7 ± 0.3	66.1 ± 3.6	5.1 ± 2.1
0.5 wt % HNT annealed	3.8 ± 0.4	66.7 ± 8,3	2.7 ± 0.4
1 wt % HNT annealed	4.0 ± 0.3	73.8 ± 7.5	4.2 ± 1.4
3 wt % HNT annealed	3.9 ± 0.2	69.2 ± 1.6	2.7 ± 0.3
5 wt % HNT annealed	3.8 ± 0.2	71.3 ± 2.5	3.2 ± 0.3
0.1 wt % SEP annealed	3.6 ± 0.3	68.6 ± 4.6	2.7 ± 0.7
0.5 wt % SEP annealed	3.6 ± 0.1	69.3 ± 1.4	3.6 ± 0.4
1 wt % SEP annealed	3.7 ± 0.2	68.3 ± 0.7	3.4 ± 0.7
3 wt % SEP annealed	3.6 ± 0.2	71.3 ± 2.5	3.2 ± 0.3
5 wt % SEP annealed	4.0 ± 0.1	66.7 ± 1.7	2.5 ± 0.1

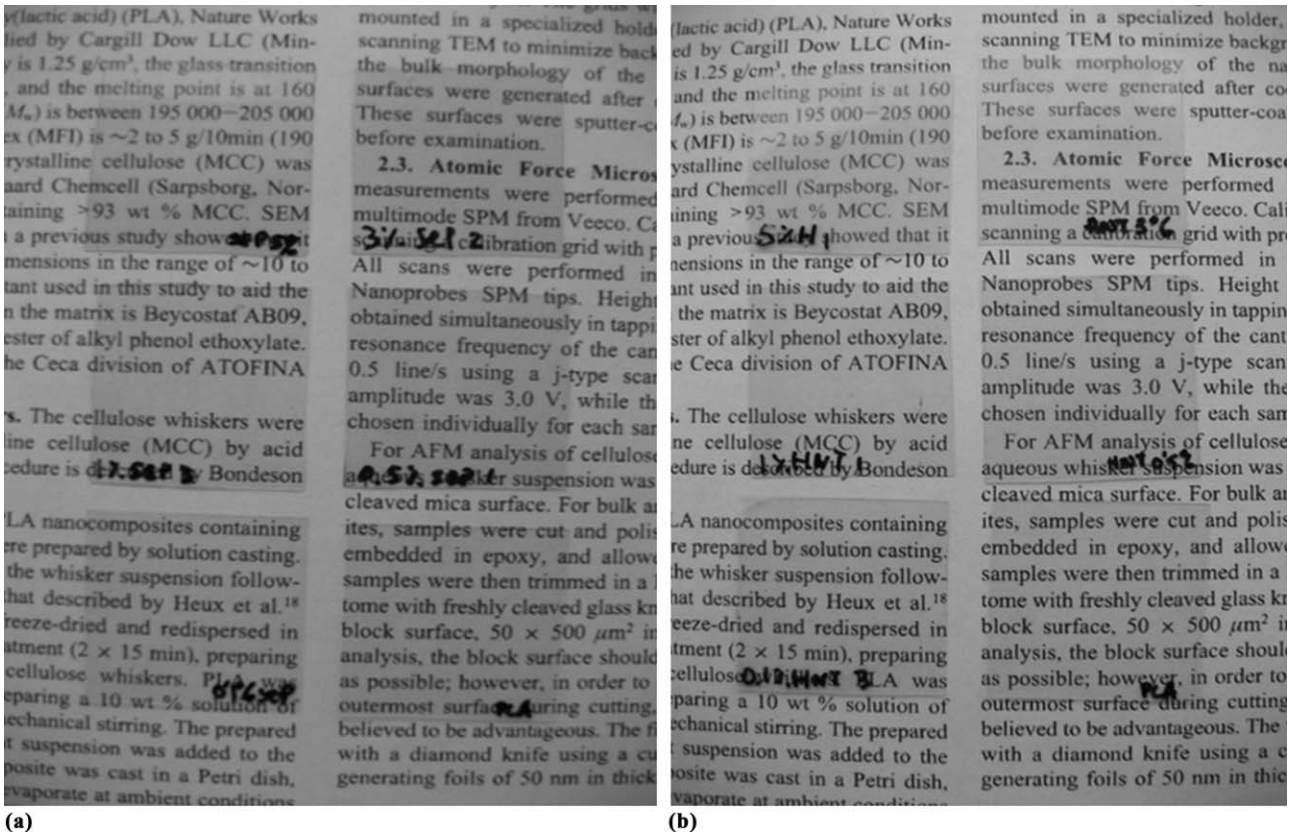

Figure 6. Translucency of (a) PLA/sepiolite and (b) PLA halloysite nanocomposite films.

optical properties. Clearly, independently of the clay type, a slight reduction of the transparency can be noted by increasing the filler loading. However, a satisfactory transparency is observed at least up to 3% by weight of clays, with a more evident loss of transparency at 5 wt % of halloysite, because of the reported lack of dispersion and formation of aggregates.

CONCLUSIONS

Melt blended compounds based on a PLA resin and two types of needle-like nanoclays were compression moulded into film samples that were systematically analyzed in terms of morphological, thermal, mechanical, and transport properties.

The research demonstrated a good dispersion of sepiolite up to 1 wt % mostly because of a good polymer–filler interaction through hydrogen bonding between the carbonyl groups of PLA and the hydroxyl groups of the filler are possible. On the contrary, halloysite's did not give an adequate dispersion for contents as low as 1 wt %.

The inclusion of nanoclays partially alter the optical transparency of the PLA films, which is important for packing applications, particularly in the case of halloysite and higher filler content.

Addition of nanoclays has only a minor effect on the degree of crystallinity. Moreover, the nucleating action of the nanofiller results to be far less effective than the annealing treatments in affecting a number of physical properties like gas barrier and tensile stiffness of considered films. Regarding the absorption measurements, as partly expected, the inclusion of clays (sepiolite) induced a relevant increase of the lag times, approximately five times higher than that of neat PLA films and a reduction of diffusion coefficients as a consequence of a more tortuous diffusion path. In case of HNT, the water absorption is slightly increased with the filler content probably because of their tubular form able to entrap water molecules.

The experimental evidences collected so far allow to appreciate the potential of the examined formulations for possible food packaging applications, although further studies may be conducted to permit more efficient design of new packaging solutions or to develop physical models of the involved phenomena.

REFERENCES

1. Holten, C. H. In Lactic Acid, Properties and Chemistry of Lactic Acid and Derivatives; Verlag Chemie: GmbH, Weinheim/Bergstr, **1971**.
2. Schopmeyer, H. H. In Lactic Acid, in Industrial Fermentations; Underkofler, L., Hickley, R. J., Eds.; Chemical Publishing Co.: New York, NY, **1954**; Chapter 12.
3. Cox, G.; Macbean, R. In Lactic Acid Recovery and Purification Systems, Research Project Series, No. 29, October, **1976**.
4. Urayama, H.; Kanamori, T.; Kimura, Y. *Macromol. Mater. Eng.* **2002**, *287*, 116.
5. Dorgan, J. R.; Janzen, J., Knauss, D. M.; Hait, S. B.; Limoges, B. R.; Hutchinsos, M. H. *J. Polym. Sci. Part B* **2005**, *43*, 3100.

6. Ikada, Y.; Jamshidi, K.; Tsuji, H.; Hyon, S. H. *Macromolecules* **1987**, *20*, 904.
7. Tsuji, H.; Ikada, Y. *Polymer* **1999**, *40*, 6699.
8. Tsuji, H.; Ikada, Y. *Polymer* **1995**, *36*, 2709.
9. Fischer, E. W.; Sterzel, H. J.; Wegner, G. *Kolloid Ze. Ze. fuer Polym.* **1973**, *251*, 980.
10. Kolstad, J. J. *J. Appl. Polym. Sci.* **1996**, *62*, 1079.
11. Picard, E.; Espuche, E.; Fulchiron, R.; *Appl. Clay Sci.* **2011**, *53*, 58.
12. Bilotti, E.; Zhang, R.; Deng, H.; Quero, F.; Fischer, H. R.; Peijs, T. *Compos. Sci. Technol.* **2009**, *69*, 2587.
13. Fischer, H. *Mater. Sci. Eng. C* **2003**, *23*, 763.
14. Morales, E.; Ojeda, M. C.; Linares, A.; Acosta, J. L. *Polym. Eng. Sci.* **1992**, *32*, 769.
15. Acosta, J. L.; Ojeda, M. C.; Morales, E.; Linares, A. *J. Appl. Polym. Sci.* **1986**, *31*, 2351.
16. Acosta, J. L.; Ojeda, M. C.; Morales, E.; Linares, A. *J. Appl. Polym. Sci.* **1986**, *31*, 1869.
17. Persico, P.; Ambrogi, V.; Carfagna, C.; Cerruti, P.; Ferrocino, I.; Mauriello, G. *Polym. Eng. Sci.* **2009**, *49*, 1447.
18. Zhou, H.; Green, T. B.; Joo, L. *Polymer* **2006**, *47*, 7497.
19. Lu, L.; Liu, H.; Xie, F.; Chen, L.; Li, X. *Polym. Eng. Sci.* **2008**, *48*, 634.
20. Tabi, T; Sajo, I. E.; Szabo, F.; Luyt, A. S.; Kovacs, J. G. *eXpress Polym. Lett.* **2010**, *10*, 659.
21. Kim, E. S.; Kim, B. C.; Kim, S. H. *J. Polym. Sci. Polym. Phys.* **2004**, *42*, 939.
22. Kopinke, F. D.; Remmler, M.; Mackenzie, K.; Mader M.; Wachsin, O. *Polym. Degrad. Stab.* **1996**, *53*, 329.
23. Wu, D.; Wu, L.; Zhang, M. *Polym. Degrad. Stab.* **2006**, *91*, 3149.
24. Rhim, J.-W.; Hong, S.-I.; Ha, C.-S. *LWT-Food Sci. Technol.* **2009**, *42*, 612.
25. Gorrasi,G.; Pantani, R.; Murariu, M.; Dubois, P. *Macromol. Mater. Eng.* **2013**, DOI: 10.1002/mame.201200424.
26. Shogren, R. *J. Environ. Polym. Degrad.* **1997**, *5*, 91.
27. Van Krevelen, D. W. In Properties of Polymers; Elsevier Science: Amsterdam, **1990**.
28. Siparsky, G. L.; Voorhees, K. J.; Dorgan, J. R.; Schilling, K. J. *J. Environ. Polym. Degrad.* **1997**, *5*, 125.
29. Cocca, M.; Di Lorenzo, M. L.; Malinconico, M.; Frezza, V. *Eur. Polym. J.* **2011**, *47*, 1073.
30. Pan, P.; Zhu, B.; Kai, W.; Dong, T.; Inoue, Y. *Macromolecules* **2008**, *41*, 4296.